A

Dissertation

on

"Chemical compatibility of glass sealants with electrolyte (8YSZ) for solid oxide fuel cell applications"

Submitted in the fulfillment of the requirements for the award of degree of

Master of Technology

in

Metallurgical and Materials Engineering

(2013-2015)

submitted by

Savidh Khan

(601302004)

under the guidance of

Dr. Kulvir Singh

(Professor)

SCHOOL OF PHYSICS AND MATERIALS SCIENCE

THAPAR UNIVERSITY

PATIALA – 147004

July 2015

CERTIFICATE

This is to certify that this dissertation entitled **"Chemical compatibility of glass sealants with electrolyte (8YSZ) for solid oxide fuel cell applications"** is submitted by **Mr. Savidh Khan** (Roll. No. 601302004) in the fulfillment of the requirement for the award of degree of Master of Technology in Metallurgical and Materials Engineering from School of Physics and Materials Science, Thapar University, Patiala (Punjab), India. It is an exclusive record of candidate's own research under the supervision of **Dr. Kulvir Singh**. This dissertation in part or full has not been submitted in any other institution for the award of such kind of degree.

Dr. Kulvir Singh
(Professor)
School of Physics and Materials Science
Thapar University, Patiala

Countersigned by:

Dr. M. K. Sharma
Professor & Head
School of Physics and Materials Science,
Thapar University, Patiala

Dr. S.S. Bhatia
Dean of Academic Affairs
Thapar University, Patiala

ACKNOWLEDGMENT

I am submitting my dissertation for the fulfillment of my 'M. Tech.' degree. This work would not have been accomplished without the support, help and guidance of a large number of people. I express my deep gratitude and respect to my supervisor **Dr. Kulvir Singh** (Professor, School of Physics and Materials Science) for his keen interest, strong motivation and constant encouragement during the course of the work. I thank him for his great patience, constructive criticism and myriad useful suggestions apart from invaluable guidance to me.

I would also like to thank **Dr. O. P. Pandey**, **Dr. Gurbinder Kaur**, **Dr. Puneet Sharma**, **Dr. B. N. Chudasama** and all other faculty members of School of Physics and Materials Science for their constructive suggestions at different stages of this work.

The meaning of my life and work is incomplete without paying regards to my respected family whose blessings and continuous encouragement have shown me the path to achieve my goals. I would like to thank to **Mr. Paramjyot Jha, Mr. Satwinder Singh, Mr. Devender Kumar, Mr Aayush Gupta, Ms Sakshi Gupta, Ms Pooja Singla, Mr Praveen Jha, Mr Gaurav Sharma, Ms Rinki** and last but not the least to **my parents** for their patience, love, moral support and constant co-operation whenever I required.

And above all, I pay my regards to the Almighty for His blessings.

Savidh Khan

Savidh Khan

CONTENTS

List of figures **Page No.**

CHAPTER 1: INTRODUCTION

CHAPTER 3: EXPERIMENTAL TECHNIQUES

CHAPTER 4: RESULTS AND DISCUSSION

List of tables **Page No.**

List of abbreviations

PAFC	Phosphoric acid fuel cell
AFC	Alkaline fuel cell
PEMFC	Proton exchange membrane fuel cell
DMFC	Direct methanol fuel cell
MCFC	Molten carbonate fuel cell
SOFC	Solid oxide fuel cell
YSZ	Yttria stabilized zirconia
CTE	Coefficient of thermal expansion
XRD	X-Ray diffraction
FTIR	Fourier transform spectroscopy
DTA	Differential thermal analysis
SEM	Scanning electron microscope
EDS	Energy dispersive spectroscopy

ABSTRACT

Four glasses are synthesized by melt quench technique. The as prepared glasses are characterized by X-Ray diffraction, Fourier transform infrared (FTIR) spectroscopy, dilatometery, differential thermal analysis (DTA) and UV-Visible spectroscopy for their structural, thermal and optical properties. All prepared samples are amorphous in nature. All the glasses are in insulating range. The highest optical band gap is 3.84 eV for CZ-4 glass. The coefficient of thermal expansion (CTE) of all the glasses is in required range for sealant in solid oxide fuel cells applications. The diffusion couple of glasses/ yttria stabilized zirconia (8YSZ) are made for interfacial study. The diffusion couples are heat treated at 850 °C for 1000 h in oxidizing atmosphere. All the diffusion couples formed smooth interface with minimum reactions at the interface. The best interface is formed between CZ-1/8YSZ diffusion couple.

CHAPTER 1 INTRODUCTION

1.1 Fuel cells

Most of the energy supply in the world satisfied by the fossil fuels and these kinds of fuels are not only non-renewable cause environmental degradation. Various environmental problems (ozone depletion, air pollution, acid precipitation, emission of radioactive substances) are the results of utilization of fossil fuels. Thus, surface temperatures have been increased at a faster rate (0.6 ^{0}C/per century). So the development of novel power generation resources has become necessary. Nowadays, fuel cells are much intersected power generation device over conventional electric power generation systems. Fuel Cell is the electrochemical device; easily convert the chemical energy into electrical energy. No mechanical work introduced in their operation therefore their efficiency is not limited by Carnot cycle. Fuel cells promise good efficiency, cost effective, fuel adaptability reliability, and negligible of green house gases emission [1].

1.2 Classes of fuel cells

These cells are categorised into different types depending upon their working temperature and the electrolytes used. The different types of fuel cells are shown in figure 1.1 [2]. The different kinds of fuel cells are listed below;

i. Alkaline fuel cell (AFC).
ii. Molten carbonate fuel cell (MCFC).
iii. Direct methanol fuel cell (DMFC).
iv. Proton exchange membrane fuel cell (PEMFC).
v. Phosphoric acid fuel cell (PAFC).
vi. Solid oxide fuel cell (SOFC).

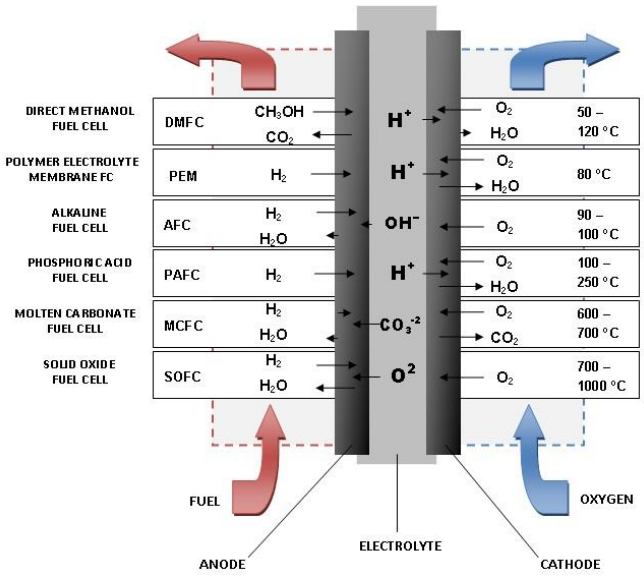

Figure 1.1: Categories of fuel cells based on operating temperature, fuel and transport ions.

The PAFC uses phosphoric acid as an electrolyte. In these kinds of cells electric power is generated by feeding hydrogen-rich and CO_2-containing reformate gas as .The working range of a PAFC stack is ~ 180-210°C and the efficiency is ~ 40-45%. The main advantage of these kinds of cells is that they are quite resistant to poisoning by carbon monoxide. However, at low temperature, carbon dioxide (CO_2) intoxication of Pt electro-catalyst is observed in the anode, since phosphoric acid exhibit poor ionic conductivity, at low temperature.

The DMFC uses methanol as a fuel. Since boiling point of methanol is 60 ^{0}C, it can be easily stored. These cells are reliable portable energy resources, being their operating temperature ~ 150 ^{0}C. In addition, Methanol is a relatively cheap liquid and is thus more attractive than hydrogen as a fuel for transportation purposes. The main losses in DMFCs are due to reaction incompletion as some surface intermediates are formed on oxidation of methanol [3]. In PEMFC ion exchange membrane is employed as an electrolyte. In these cells the corrosion problems are minimal. The main disadvantage of these cells is water management, since the electrolyte employed in them should remain hydrated all the time. Additionally, PEFCs are sensitive to

poisoning by CO, sulphur and ammonia [4]. Alkali fuel cells exhibit extremely high power densities but removal of carbon dioxide from both the fuel and oxidant side in order to prevent the formation of non-conducting alkali carbonates after the reaction with CO_2 makes them user unfriendly [5]. MCFC uses molten carbonate salt, which is suspended in a ceramic matrix with porosity as an electrolyte material. The high operating temperature (~ 650 ^{0}C) increases the reaction kinetics and eliminates the need of Pt catalyst. The main disadvantage associated with MCFC is the usage of liquid electrolyte rather than a solid which increases the chances of corrosion in these fuel cells. High temperature solid oxide fuel cell comprises of a solid oxide ion conducting electrolyte. Because of the high operating temperature and solid electrolyte SOFCs offer many advantages over the cells discussed above. Presently, fuel cells are being used on large scale; PEMFCs are used in transportation whereas SOFCs are employed in high power generation intentions.

1.3 Solid oxide fuel cells (SOFC)

SOFC can be the best possible candidate to increase the energy supply in an eco-friendly manner. During SOFCs operation only water and heat is generated as a byproduct along with electricity. The efficiency of SOFCs can reach up to 65% with regeneration. Therefore, these can be considered as clean and efficient source of energy. Another advantage of SOFCs is fuel flexibility. Any kind of hydrocarbon can be used as fuel for SOFC operation. The reformation of hydrocarbons to hydrogen gas can take place inside the cell. Thus, solid oxide fuel cells (SOFCs) can be cost effective and viable energy source in near future. However, the main limitation of SOFCs is its high working temperature, which reduces lifetime of these devices. Thus, to improve the lifetime of these devices the idea is to reduce working temperature. Working temperature depends on the electrolyte employed in them [6-10].

1.4 Design of SOFCs

Based on their geometry, power density and method of sealing the SOFC can be categorised in two category; (i) external supporting and (ii) self-supporting. In type first category, the single cell is set up of porous substrate or thin layers on interconnect. In type second category, type of a single cell, one component of the cell works like a cell supportive. Hence, single cells may be planned as components supported to SOFC [11, 12]. Single SOFC cell generates small electric potential ~ 0.70 V. Therefore, to obtain the workable outputs of power for single cell is combined for making a fuel cell stack. The following types of stack designs are most popular:

1.4.1 Tubular design

Tubular SOFCs were pioneered in 1960s. Nowadays, tubular configuration of SOFC is the main attraction among other SOFC configurations because the tubular configuration eliminates the need of gas seals. The power density of the tubular cells depends upon the inverse of cell diameter, narrower the tube better is the performance of the cell.

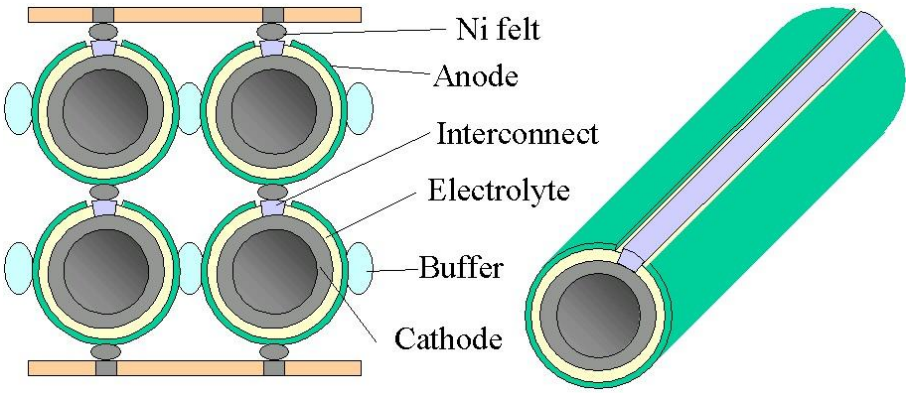

Figure 1.2: Schematic for a tubular SOFC design.

But on the similar grounds more is the area of the cell more will be its performance. Therefore, the optimization between length and diameter of cell should be done in a way, that ohmic losses in a cell occurring due to longer path than other fuel cells are least [13, 14]. The schematic for a tubular SOFC is shown in figure 1.2.

1.4.2 Planar design

Planar design of SOFC is the cheapest and easiest to fabricate and perform. In this type of configuration the three components electrode, electrolyte and cathode are stacked on each other. Planar SOFCs produce higher power density (~ 1 MW m^{-3}) than tubular SOFC, but the major demerit of planar SOFC is the requirement of sealing during fabrication and operation of cell. As the gas leakage occurs at higher temperature [15]. The schematic for a planar SOFC is shown in figure 1.3.

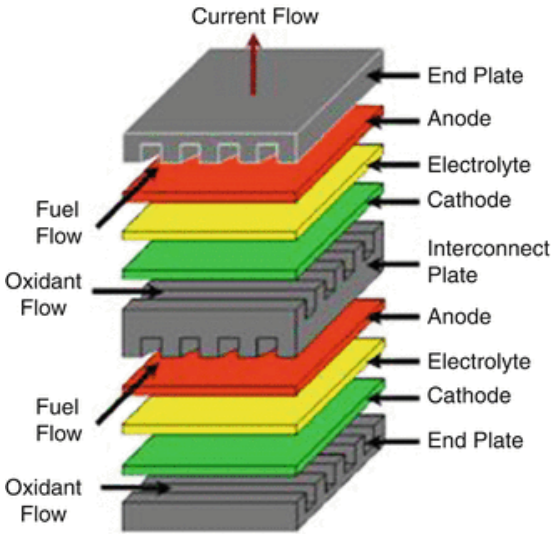

Figure 1.3: Schematic for a planar SOFC design.

1.5 Components of SOFCs

The main components employed in a cell are irrespective of the kind of configuration of cell. The schematic for SOFC components is shown in Figure 1.4. The properties of these components along with requirements are as follows:

1.5.1 Anode

Anode acts an electrode from where the fuel is fed into the cell. At present, a cermet composed of an ion conducting phase (YSZ) and metallic phase (Ni) is used as an anode. For the better performance of the cell it is required that the contact line between Ni (electronic conductor),

YSZ (ionic conductor) and the gas phase called "triple phase boundary" is large. The performance of anode depends on its microstructure and precursor powders. The relative size of the YSZ particles should be smaller than Ni particles to minimize the degradation. But the main drawbacks of Ni/YSZ material are its low sulphur tolerance, poor redox stability, nickel coarsening after long term operation and carbon deposition when using hydrocarbon as fuel. Some new materials like Cu-CeO_2- YSZ/ SDC have also developed as anode material to enhance the performance of cell [16, 17].

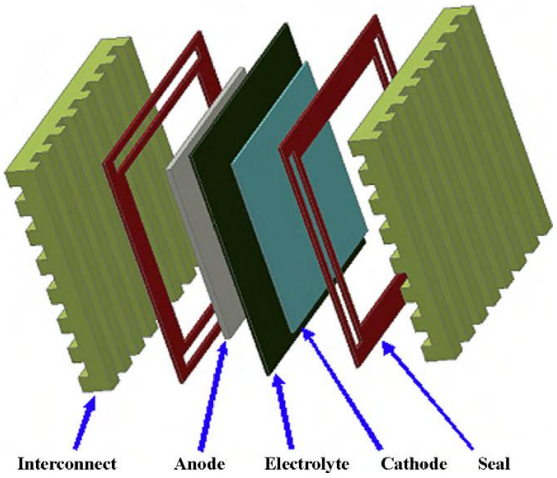

Figure 1.4: Schematic for components of SOFC.

1.5.2 Cathode

The cathode/air electrode is an electrode in SOFC, where reduction of oxygen gas takes place. Transportation of air takes place at cathode side to anode side through electrolyte. Cathode should represent high electronic conductivity and porosity to allow the oxygen ions diffusion. It must be stable under oxidising environment. Sometimes, activation loss, made by the kinetics of O_2 reduction occurring at cathode limits the performance of SOFC. Strontium doped lanthanum manganite (LSM) is used conventionally, as cathode to reduce the over potential losses. It has been observed that maintaining its porosity while decreasing the grain size can increase current density by decreasing the over potential losses. Hence, smaller grains on inner layers and larger

grains multi-layered cathodes on outer layers can be increased the working efficiency of SOFCs [18, 19].

1.5.3 Sealant

In case of planar SOFCs high temperature sealants at the edges of components of cell, between the stack of fuel and the gas multitude are required for prevent direct combustion of fuel. For an effective sealing a sealant must be airtight, during thermal cycling. Leakage on small level in the seal can have adverse effects on the cell potential and can reduce the cell performance. Stability in oxidising and reducing atmosphere as well as compatibility with the cell components is necessary condition for glass sealants. Coefficient thermal expansion (CTE) of sealants is another aspect, which should be taken care of. The TEC of all the components employed in SOFC must be matching. Commonly, alkaline earth and alkali containing glass sealants are used and are expected to operate at above 1000 h without degradation. The main problem associated with alkali metal glass and glass- ceramics is that they can react with other components during fuel cell operation [20, 21].

1.5.4 Interconnect

As discussed earlier in order to obtain a voltage output for practical application several cells are stacked. These cells are connected either in series or parallel with the help of interconnects. Interconnect provides the electrical connection between the cathode of one cell and anode of another cell. Thus, interconnect must be highly electronically conducting. So that ohmic losses generated as a result of interconnect are small and the power density remains unaffected. It also uses to prevent the mixing of two gases [22-24].

1.5.5 Electrolyte

To maintain the electrical efficiency of the fuel cells the conduction of ions from one electrode to another takes place through the electrolyte. Depending on the conducting ion specie, there are three kinds of electrolytes such as protonic, anionic and mixed ionic. However, mostly oxide ion conducting electrolytes are used for high temperature SOFCs [25]. The properties of electrolytes also depend on its crystal structure, amount of doping and its chemical stability with other components of SOFC. Mostly YSZ is used as electrolyte material for SOFCs. It represents high ionic conductivity and good stability under both oxidising and reducing atmospheres [26]. But the main limitation of YSZ is the high operating temperature. Scandia doped zirconia (ScSZ) can also be used as electrolyte but it represents the thermal aging and hence reduction in conductivity. Another limitation of ScSZ is the purity and availability of scandium oxide [27]. Bismuth based systems can also be a good candidate for electrolytic applications in SOFCs. Since, it represents high ionic conductivity in intermediate temperature ranges.

1.5.6 Basic characteristics of electrolyte

Good electrolyte is supposed to have crystal structures with open channels, layers to provide pathways for easy ionic transport via hopping mechanism. High conducting electrolytes are required to fulfil the following conditions:

1) Availability of large number of free ions for the greater conduction of oxide ions
2) It should be stable at high temperature.
3) 3D networking through open channels for the migration of ions.
4) Large number of vacancies for hopping as well as same energies of the occupied and vacant sites.
5) Coefficient of thermal expansion must be comparable to the others components cell at working temperature of cell.

6) Negligible chemical interaction with electrode of fuel cell.
7) High density to promote gas impermeability.

1.6 Why seals are required?

The development of suitable sealing materials for high temperature SOFCs applications is the big task all around the world to separate the fuel and air. It is used to prevent the mixing of gaseous fuel (H_2, CO_2, CH_4) and air and leakage of fuel into air during operation will cause to direct combustion and might cause of local overheating with decreasing efficiency. Thus for the commercialization of SOFCs, a, suited sealing material is needed. The rigorous necessities of this sealing material are good air tightness, good adhesion with various cell components such as electrolyte, anode, cathode, electrical insulation and interconnect chemical compatibility. Thermal and chemical properties in a seal material should be obtained at the same time for solid oxide fuel cell operation. CTE of a sealing material should be matching the other components of SOFCs. It is the necessary condition to make the interface crack free, nonporous for a perfect sealant.

1.7 Required properties for sealing materials

A sealing material must satisfy the following properties so that it can be resist longer time in rigorous condition without degrading SOFC components [28-30].

1) Good adhesion of the seal material with the components of SOFC.
2) CTE of seal material should be match with the components of the SOFC.
3) High electrical resistivity .
4) Minimum diffusion and volatilization of the sealant material components.
5) Thermal stability with morphological stability at the working temperature of SOFCs.

6) Highly thermal shock resistance.
7) Free from defects (pores, micro cracks, bubbles)
8) Availability and low cost.

Hence, the selection of sealing materials is very important for stacking the one unit of cell to another. It can be depended on a number of configurationally factors such as thermal gradients required throughout the seal and components of SOFCs, individual cell and stack materials, maximum volume and weight of the power plant, expected required heating and cooling rate of the device.

1.8 Types of sealing materials

There are three types of sealing materials such as compressive, compliant bonded and rigid bonded/glass seals. Deformable material used as a compressive seal does not show the good bonding to components of planar solid oxide fuel cell. Mica and mica based hybrid materials can be used as compressive seals for SOFCs technology. These kinds of seals are costly and complex in design [31]. Compliant bonded seals such as metal-brazes have been deformed plastically at room or above temperature. This diminishes the requirement of CTE matching between the SOFCs components [32-34]. On the other hand compliant bonded seals are not much suited for SOFCs due to the following reasons:

- Poor bonding with the SOFC component.
- Hydrogen embrittlement.
- Electrical conductivity.
- Prone to oxidation.

The glass seal comes in the class of rigid bonded seals. The joint which made by the glass seals do not deform at room temperature. It can easily glue the cell components together. Presently, SOFC technology is focused on the development of the rigid bonded seals (glass, glass-ceramics). Glass seal can be considered as a good option for SOFC due to its stability to longer duration of time (5000-40,000 h) at high temperatures (600^{o}C to 900^{o}C). Glass seals show many advantages over the compliant and compressive seals which are as follows [35-37]:

- Rigidly bonded to the SOFC components.
- Electrically insulating nature.
- Easy to fabricate.
- Flexible in design.
- Low cost

1.9 Glasses as sealant

Glass and glass-ceramic seals are electrically insulating, can prevent the mixing of gases inside the cells and leakage into the air. Additionally, these types of seals are very easy to manufacture, cost-competitive and flexible in design [38-42]. A glass/glass-ceramic seal accomplishes a broad range of the properties, which needed for seals in SOFCs by desirable compositional design. There are some crucial properties to a glass seal material i.e. (CTE), devitrification resistance T_s and T_g. During the operation of the cell, the value of a glass transition temperature (T_g) of glass seals should be marginally below the cell working temperatures [43]. Generally, T_g and softening temperature (T_s) of glass seals increase with SiO_2 content due to higher amount of bridging oxygen. Network connectivity decreases with the higher amount of non-bridging oxygen and hence T_g and T_s Presence of planar boroxyl structural units in B_2O_3 containing glass and low

glass transition temperature (275 °C) lead to low T_g. A seal glass normally consists of glass former, modifier and intermediate. Glass seals generally have 20-45 mol% network modifier and 5-10 mol% intermediate oxide. Some additives (transition metal oxides and rare earth metal oxides) are also used in glass seal compositions to improve the thermal properties of glasses. To increase glass transition temperature (T_g) of a seal glass by 30-50°C less than 10 mol% La_2O_3 is enough though more than 20 mol% has been used in some seal glasses [44]. T_g and T_s of a seal glass can be increased and decreased /unchanged according to the working style of these oxides. T_g and T_s is decrease, or remain unchanged when these oxides are work as modifiers and is increased when these oxides work as formers.

To get crack-free interface, the coefficient of thermal expansion of glass seals should not differ by more than 1×10^{-6}/°C from the components of SOFC. Devitrification is undesirable as it go down some of useful glass seal properties. The basic reasons for devitrification of a glass seal are heterogeneity in glass network structure, the small nuclei shaped on glass making, residual stress from mechanical polishing and surface flaws. Glass former degrades the devitrification resistance of seal glasses in two ways. The network connectivity decreases with increases non-bridging oxygen within the glass systems. Presence of various different structural units accelerates heterogeneity in glass systems [45]. Borate glass systems show lower degree of devitrification resistance than Silicate glass sytems. Devitrified phase is of most concern due to CTE difference between the components. Lower flow ability and stresses of the devitrified phases can be created cracks in glass seal at the interface.

1.10 Interfacial compatibility of glasses with electrolyte

To understand the composition related structure property of glass seal is necessary requirement to find a suitable seal glass for SOFC. Various glass systems with required properties have been

discovered, but longer time stability always remains a big problem. The performance and durability of SOFC depends upon the thermal and mechanical properties (interfacial strength) of a seal glass. Glass seal shows wetting and bonding with SOFC components to form beneficial sealing without any pores and cracks at the interface. The interaction takes place between interfacing SOFC components and glass seal through chemical reaction and inter-diffusion of the constituents of the glass seal [46, 47]. Normally, glass seals show great wetting with ZrO_2 electrolyte. So, there is no problem with ZrO_2 electrolyte in reference to interfacial stability with a seal glass. Glass seals with the interaction of YSZ electrolyte form $CaZrO_3$/$SrZrO_3$/$BaZrO_3$ [48]. Glass seals with alkali oxides are not desirable because as a result alkali silicate glasses may be easily reacted with SOFC components. Alkali chromates such as K_2CrO_4 and Na_2CrO_4 are formed, which destabilized glass network. At the cell operating temperature, Interfacial interaction study of SOFC components such as anode, cathode, electrolyte, interconnect and sealant is very significant to recognize the different phase formations. The nature and volume of the resultant phases may cause reduction of the life SOFC. On the other hand, little consideration is paid to the chemical interaction between the sealants interfaces and low temperature electrolyte. At the same time, some additional work is needed to determine the undesirable effect of this interaction, which leads to inter-diffusion, reduced electrochemical activity of cell components and degradation of SOFC performance.

The present work is focused on the chemical compatibility of glass sealant with electrolyte (8YSZ) for SOFC application for achieving the long term operation goal. In the present investigation, efforts are being made to understand the mechanism of interfacial interaction and their effect on crystallization kinetics, formation of various crystalline phases and their effect on thermal expansion and structural properties.

References

1. B. Ku, Y. Zhang, J. Univ. Sci. Technol. B. 15(1) (2008) 84.
2. B. C. H. Steele, A. Heinzel, Nature 414 (2001) 345.
3. K. Sundmacher, T. Schultz, S. Zhou, K. Scott, M. Ginkel, E. D. Gilles, Chem. Eng. Sci. 56 (2) (2001) 333.
4. E. Gulzow, Fuel Cells 4 (2004) 251.
5. K. Takizawa, Molten carbonate fuel cells- Vol II, Encyclopedia of Life Support Systems.
6. M.S. Dresselhaus, I. L. Thomas, Nature 332 (2001) 332.
7. B. C. H. Steele, H. Angelika, Nature, 345 (2001) 414.
8. R. B. Cervera, Y. Oyama, S. Yamaguchi, Solid State Ionics 178 (2007) 569.
9. S. M. Gheno, V. L. Pimentel, M. R. Morelli, P. I. F. Paulin, Microscopy and Microanalysis 19 (2013) 688.
10. A. B. Stambouli, E. Traversa, Renew. Sust. Energ. Rev. 6 (2002) 433.
11. S. P. S. Badwal, K. Foger, Ceram. Int. 22 (1996) 257.
12. N.Q. Minh, Solid State Ionics 174 (2004) 271.
13. K.S. Howe, G. J. Thompson, K. Kendall, J. Power Sources 196 (2011) 1677.
14. C. Rayment, S. Sherwin, Introduction to fuel cell technology, Department of Aerospace and Mechanical Engineering, University of Notre Dame USA (2003).
15. A. Cubero, J. I. Pena, M. A. Laguna-Bercero Appl. Surf. Sci. 335 (2015) 39.
16. C, Suciu, A.C. Hoffmann, E. Dorolti, R. Tetean, Chem. Eng. J. 140 (2008) 586.
17. C. Sun, R. Hui, J. Roller, J. Solid State Electrochem. 14 (2010) 1125.
18. V. M. Janardhanan, O. Deutschmann, Z. Phys. Chem. 221 (2007) 443.
19. K. L. Ley, R. Kumar, J. H. Meiser, I. Bloomc, J. Mater. Res. 11 (6) (1996) 1489.

20. J. W. Fergus, J. Power Sources 147 (2005) 46.

21. W.Z. Zhu, S. C. Deevi Mater. Sci. Eng. A 348 (2003) 227.

22. J. W. Fergus, Mate. Sci. Eng. A 397 (2005) 271.

23. J. W. Fergus, Solid State Ionics 171 (2004) 1.

24. M. L. Faro, D. L. Rosa, V. Antonucci, A. S. Arico, J. Indian Inst. Sci. 89 (4) (2009) 363.

25. A. Tarancón, Energies, 2 (4) (2009) 1130.

26. V. V. Kharton, F. M. B. Marques, A. Atkinson, Solid State Ionics 174 (1-4) (2004) 135.

27. A. Goel, E. R. Shaaban, D. U. Tulyaganov, J. M. F. Ferreira, J. Am. Ceram. Soc. 91 (2008) 2690.

28. J. Tong, M. Han, S. C. Singhal, Y. Gong, J. Non-Cryst. Solids 358 (2012)1038.

29. H. T. Chang, C. K. Lin, C. K. Liu, S. H. Wu, J. Power Sources 196 (2011)3583.

30. J. Duquette, A. Petric, J. Power Sources 137 (2004) 71.

31. Y. S. Chou, J. W. Stewen, G. G. Xia, Z. G. Yang, J. Power Sources 195 (2010) 566.

32. Y. S. Chou, J. W. Stevenson, P. Singh, J. Electrochem. Soc. 154 (2007) B644.

33. J. Y. Kim, J. S. Hardy, K. S. Weil, J. Mater. Res. 20 (2005) 636.

34. K. S. Weil, J. Miner, Met. Mater. Soc. 58 (2006) 37.

35. J. W. Fergus, J. Power Sources 147 (2005) 46.

36. P. A. Lessing, J. Mater. Sci. 42 (2007) 3465.

37. S. Ghosh, A. D. Sharma, A. K. Mukhopadhayay, P. Kundu, R. N. Basu, Int. J. Hydro. Energy 35 (2010) 272.

38. V. Kumar, Rupali, O. P. Pandaey, K. Singh, Int. J. Hydro. Energy 36 (2011) 14971.

39. M. K. Mahapatra, K. Lu, Int. J. Appl. Cera. Tech. 7 (2010) 10.

40. F. Smeacetto, M. Salvo, M. Ferraris, J. Cho, A. R. Boccaccini, J. Euro.Cera.Soc. 28 (2008) 61.
41. C. Lara, M. J. Pascual, A. Duran, J. Non-Cryst. Solids 348 (2004) 149.
42. P. Herma. W. T. Han, A. R. Cooper, J. Non-Cryst. Solids 102 (1988) 88.
43. M. K. Mahapatra, K. Lu, J. Mater.Sci. 44 (2009) 5369.
44. J. Deubener, J. Non-Cryst. Solids 351 (2005) 1500.
45. J. M. Howe, Int. Mater. Rev. 38 (1993) 233.
46. J. M. Howe, Int. Mater. Rev. 38 (1993) 257.
47. K. A. Nielsen, M. Solvang, S. B. L. Nielsen, A. R. Dinesen, D. Beeaff, P. H. Larsen, J. Euro. Cera. Soci. 27 (2007) 1817.
48. K. Ogasawara, H. Kamedea, Y. Matsuzaki, T. Sakurai, H. Yokokawa, J. Electrochem. Soc. 154 (2007) B657.

The making a suitable sealing materials for making SOFCs is a challenge. Formation of crystalline phases at the interfacing components resulting change in CTE is a big problem. However, glass along with glass ceramics can act as good sealants for SOFCs. Interfacial study for longer duration of time in both oxidizing and reducing environment is necessary. In this chapter, the interaction study among the glass sealants and components of SOFCs such as electrolyte is discussed.

Chou *et al.* [1] have studied NiO effect on the characteristics of Ca-Sr-Ni-Y-B system. They have made the sealant material in two ways: composite glass and glass making. They observed that CTE of glass decreased on large scale with higher NiO content where as the CTE increased with change in volume of NiO for composite glass. They also found that higher content of NiO in glass resulted into the formation of precipitates. Hence formed powder compact of glass exhibited cracks of wide range. It was reported that glass-based composite with high NiO content (15 vol.%) was fracture free. In their other report [2], composite glass having change in NiO content (10%) was analyzed. It was observed that the glass is very supportive to the SOFCs component like YSZ electrolyte, Ni/YSZ anode and metallic interconnect (Crofer22APU) at several temperatures. Samples do not lose their hermiticity at the highest temperature (1050 ^{o}C), in reducing atmosphere and 10 thermal cycles. It was observed that there were no reactions at the interfaces of glass/YSZ, and at last, it was conclude, that with 10 vol.%. NiO content composite glass is a good SOFC sealing material.

Goel *et al.* [3] analyzed alkaline-earth aluminosilicate glass-ceramics (GCs) as a sealant material for SOFCs. They observed that GC system's electrical conductivity decreases by adding BaO and on the other hand, BaO comprising GCs depicted higher CTE than BaO free GCs. It was

observed that there was hardly any growth of $BaCrO_4$ at the interface in between GC and interconnects diffusion couples due to Ti and Mn oxide segregation at interconnect (Crofer22 APU alloy). They conclude that due to well match CTE, good adhesion between interconnect and electrolyte GC is a good option for SOFC applications.

Hao *et al.* [4] synthesized three glass systems namely $SrO\text{-}SiO_2\text{-}Al_2O_3$, $SrO\text{-}CaO\text{-}SiO_2\text{-}Al_2O_3$, and $BaO\text{-}CaO\text{-}SiO_2\text{-}Al_2O_3$. It was observed that under low loading condition $24SrO\text{-}16CaO\text{-}25SiO_2\text{-}8Al_2O_3$ glass system is best sealant for SOFC without leakage. It was also observed that in reference to air tightness, SrO comprising glass system exhibits the best wetting in comparison to other system due to the SrO i.e. decreased the contact angle between crofer22 APU and glass.

Park *et al.* [5] examined the activation energy for recrystallization and frequency parameter of $MgO\text{-}CaO\text{-}SiO_2\text{-}P_2O_5\text{-}F$ glass system using Differential Thermal Analysis (DTA). It has been found that by raising content of TiO_2, the kinetic parameter at crystallization phase, wollastonite & apatite, showed change. Hence, it is an effective way to encourage the crystallization of wollastonite and apatite. It was concluded that friction coefficient and wear rate decreased with addition of TiO_2 into to base of glass.

Singh *et al.* [6] examined $SiO_2\text{-}MgO\text{-}B_2O_3\text{-}Y_2O_3\text{-}Al_2O_3$ glass systems and found that the crystallization behavior was affected on large scale of these glasses by the addition of yttrium oxide (Y_2O_3). The T_g, T_c and glass stability increased with by adding Y_2O_3 content.

Yang *et al.* [7] investigated the interaction of $35BaO\text{-}15CaO\text{-}5Al_2O_3\text{-}10\ B_2O_3\text{-}35SiO_2$ glass system with alumina and chromia-forming alloys. For all chromia forming alloys, chromium got dissolved in this glass seal and made a solid solution with enriched chromium. On the other hand, pores in the seal could be seen without any growth of barium chromate in alumina-forming

alloys. It was also observed that these glass ceramic showed good chemical compatibility with electrolyte (YSZ).

Kumar *et al*. [8] studied glass system of SiO_2-B_2O_3-MgO/SrO-A_2O_3 (A=Y, La, Al) for making SOFC using several techniques like XRD, Dilatometer and FTIR spectroscopy. They found that MgO contained glasses, which were prepared by doping of Al, La, and Y indicated greater crystallization temperature (T_c) in comparison to SrO contained glasses. It may accounted because of lower field strength of Sr^{2+} than Mg^{2+} cation. They also found that SiO_2-$20B_2O_3$-$30SrO$-$10Y_2O_3$ glass system shows higher thermal expansion in comparison to other glass systems and comparable with components of SOFCs, hence it can be used as a good sealant for SOFCs.

Mahapatra *et al.* [9] discussed required properties and compositional challenges for the three types of glasses such as borate, silicate and borosilicate glass. It was observed that all three samples satisfied the required thermal properties but silicate glasses shown better devitrification resistance as compared to other glass seal. In reference to the long term stability, seal glass of borate and borosilicate was not desirable due to vaporization occuring in the cell operating environment. It was also observed that Borosilicate glasses are important for facilitation of interconnect bonding but put down the stability of interface. A seal glass of SrO-La_2O_3-Al_2O_3-SiO_2 has shown remarkable characteristics such as, sealing execution, thermal cycling resistance, desired thermo-chemical properties and as compared to others seal glass. It has been observed that the origin of thermo-mechanical stress between the sealing material and the components of the SOFCs was mismatch of young modulus & coefficient of thermal expansion.

Ley *et al.* [10] have developed a family of sealants ($SrO\text{-}La_2O_3\text{-}Al_2O_3\text{-}B_2O_3\text{-}SiO_2$) for use in the high temperature SOFC. It has been found that CTEs ($8\text{-}13 \times 10^{-6}$ /° C) of these materials exhibit a good correspondence with that of the SOFC components. It has been observed that this sealant bonds well with the ceramics of the SOFC.

Ghosh *et al.* [11] have prepared several systems of ceramic-glass such that $RO\text{-}Al_2O_3\text{-}SiO_2$ (R=Ba, Ca) for planar anode-supported IT-SOFC (800 °C). The crystallization behavior and bonding characteristics along with electrical, thermal, and chemical properties of the glass ceramics of parent glasses with (YSZ) electrolyte and interconnect Crofer22APU. It has been studied that the T_g of the prepared glasses was in the range of 600-635 °C. It has also been reported that the CTE can be tailored between that of YSZ and Crofer22APU by varying the alkaline-earth metal content. Glass seal showed CTE matching with Crofer22APU and i.e.10-13 /° C.

Nonnet *et al.* [12] presented two types of seals: glass and glass ceramic. High content of silica alkali borosilicate glass could satisfy the required properties for a seal. It could be used as effective seal at 800 °C for both metals and ceramics without any cracks. It could also be used to hold seal at the time of thermal cycling. It could be operated effectively up to 100 hrs without much crystallization. On the other hand, they investigated two glass compositions containing 6 wt. % B_2O_3 and thermal transient endurance is tested by measurement of CTE.

Kaur *et al.* [13] studied $AO\text{-}SiO_2\text{-}B_2O_3\text{-}Y_2O_3$ (A = Ca, Sr, Ba) glass systems and observed that the sealing temperature of all the glasses lies between SOFC operating temperature (800-1000 °C). It was observed that CaY glass seal show higher stability with low free volume and nucleating sites. CaY system has highest activation energy of crystallization along with higher

stability, lower rate of crystallization and lower abrupt change in coefficient of thermal expansion than other glass. It has been observed that the coupling between CaY glass sample and Crofer22APU, which is treated with heat at 850°C, for 50 hrs, showed good adhesion at interface. Finally, they concluded that that CaY glass exhibit good potential to work as sealant in solid oxide fuel cell. In another report [14], they have discussed the diffusion couples formed from lanthanum-based barium borosilicate glass at different range of temperature of electrolytes. It was found that glass is having higher devitrification resistance for heat treatment up to 100 hrs. The phase of $BaSiO_3$ was obtained for both the glasses after 750 hrs treatment whereas there is no formation of zirconate phase. It was obtained that the pore size is maximum during heating of 5 hrs and decreased with the increase in duration of heat treatment resulting in BL glass self healing capacity. It was observed that the diffusion couples show good characteristics of bonding.

Kumar *et al.* [15] optimized yttrium based borosilicate glasses and found that these glasses show good capability of bonding with YSZ, without any formation or delamination of zirconate in any diffusion couple. All the diffusion couples showed smooth interfaces after thermal cycling. They suggested that glasses of CaY were more appropriate for application as sealant in comparison to other prepared glasses.

Ghosh *et al.* [16] investigated various glass systems having SiO_2, B_2O_3, BaO, MgO and CaO oxide content. They evaluated the performance of the sealants in short stacks (up to 6-cell) of SOFC for 20 days. They observed the open circuit voltage of the stacks and found it close to the expected values and it remained same during the period of stack testing and verified its potential application for SOFC.

Lin *et al*. [17] prepared borosilicate glass ($BaO\text{-}SiO_2\text{-}B_2O_3$, $BaO\text{-}SiO_2\text{-}B_2O_3\text{-}Al_2O_3$) systems for IT-SOFCs. They characterized its CTE, glass forming ability, crystalline phases and thermo-chemical stabilities. The most encouraging result was glass can be fully wetted with different components at 1000°C sealing temperature & CTE. They conclude that glass remained amorphous after 5000 hrs test and was found to be stable under these conditions as well as compatible with other components of fuel cell.

References

1. Y. S. Chou, J. W. Stevenson, R. N. Gow, J. Power Sources 168 (2007) 426.
2. Y. S. Chou, J. W. Stevenson, R. N. Gow, J. Power Sources 170 (2007) 395.
3. A. Goel, D. U. Tulyaganov, V. V. Kharton, A. A. Yaremchenko, J. M. F. Ferreira, J. Power Sources 195 (2010) 522.
4. J. Hao, Q.Zan, D.Ai, J.Ma, C. Deng, J. Xu, J. Power Sources 214 (2012) 75.
5. J. Park, a. Ozturk, ThermochimicaActa 470 (2008) 60.
6. K. Singh, N. Gupta, O.P. Pandey, J. Mater Sci. 42 (2007) 6426.
7. Z. Yang, G. Xia, K. Scott Well, J. W. Stevenson, K. D. Meinhardt, J. Mater. Engg.Perf. 13 (2004) 327.
8. V. Kumar, Rupali, O.P. Pandey, K. Singh, Int. J. Hydro. Energy 36 (2011) 14971.
9. M. K. Mahapatra, K. Lu, J. Power Sources 195 (2010)7 129.
10. K. L. Ley, M. Krumpelt, R. Kumar, J. H. Meiser, I. Bloom, J. Mater Sci. 11 (1996) 1489.
11. S. Ghosh, A. D. Sharma, P. Kundu, R. N. Basu, J. Electrochem. Soc. 155 (2008) B473.
12. H. Nonnet, H. Khedim, F.Mear, J. Aust. Ceram. Soc. 48 (2012) 205.
13. G. Kaur, V. Kumar, O. P. Pandey, K. Singh, J. Electrochem. Soc. 159 (2012) B.
14. G. Kaur, O. P. Pandey, K. Singh, Int. J. Appl. Ceram. Technol. 11 (2012) 1.
15. V. Kumar, G. Kaur, K. Lu, O. P. Pandey, K. Singh, Int. J. Appl. Glass Sci. 5 [4] (2014) 410.
16. S. Ghosh, A. D. Sharma, P. Kundu, R. N. Basu,Trans. Ind. Ceram. Soc. 67[4] (2008) 161.
17. S. E. Lin, Y. R. Cheng, W.C.J. Wei, J. Europ. Ceram.Soc. 31[11] (2011) 1975.

CHAPTER 3 EXPERIMENTAL TECHNIQUES

The particulars of sample processing and characterization techniques which were followed during the course of the present investigations are presented in this chapter.

3.1. Glass sample preparation:

Glasses were developed by mixing the following chemicals SiO_2, B_2O_3, Y_2O_3, CaO and ZrO_2 with regular smelt-quench technique. The purity of elemental oxides that used to develop the samples was ≥ 99 %. All the chemicals were procured from Sigma Aldrich or CDH India. All groups were developed by mixing a proper mole division of required original constituent. Compositions of sample with their tag are tabulated in 3.1.

Table 3.1: Compositions (mol%) by their labels.

Sample ID	CaO	ZrO_2	Y_2O_3	B_2O_3	SiO_2
CZ-1	20	10	10	30	30
CZ-2	22.5	7.5	10	30	30
CZ-3	25	5	10	30	30
CZ-4	27.5	2.5	10	30	30

For every composition, needed quantity was taken in accordance with stoichiometry ratio. The muddles were pulverized to smash the lump mass. Following pulverizing, the powder were transferred to re-crystallized melting pot and liquidized at high temperature heating system. The compositions were initially heated at 1000ºC for 2 h to facilitate the calcination. During calcination moisture is released. Then the compositions were melted at 1550 ºC and soaked for 1.5 h to achieve homogeneous slurry. The flow chart explains the procedure of sample development and characterization (figure 3.1).

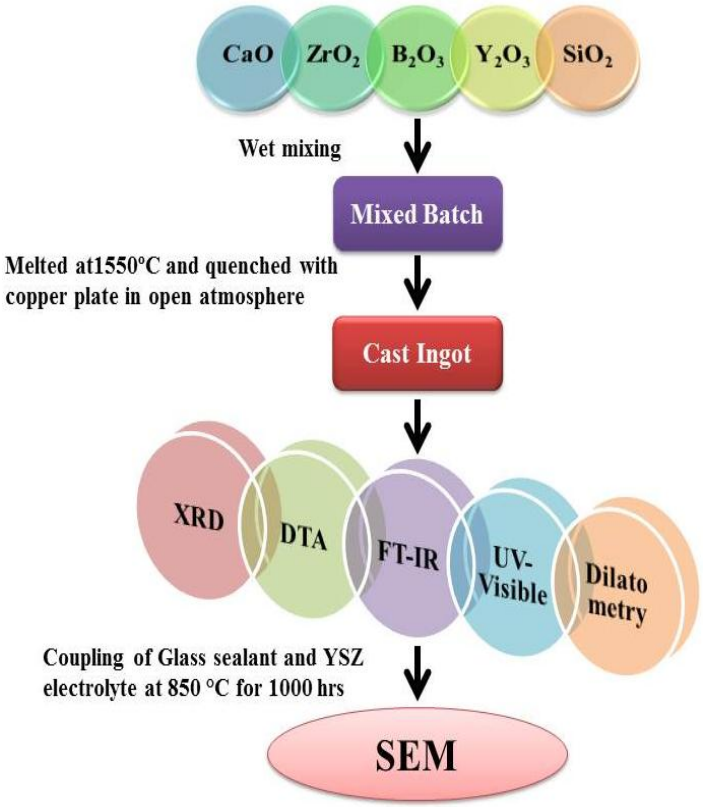

Figure 3.1: Flow chart describing preparation and characterization of glasses.

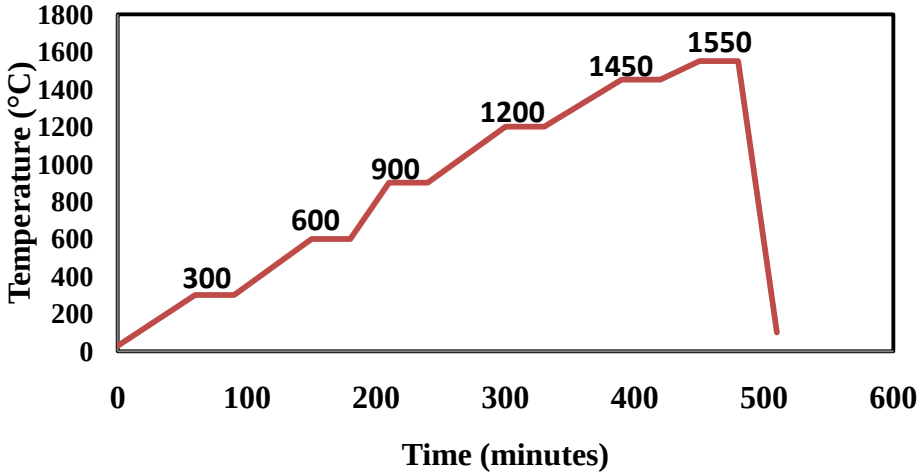

Figure 3.2: Heating rate followed for glass making.

The remained melt was discharged on a leveled Cu plate for quenching covered by another copper plate at open atmosphere. All the glasses were developed with this same route as briefed on top. The schedule followed for melting of samples is also shown in figure 3.2.

3.2. Electrolyte synthesis

In the present study, Yttria stabilized zirconia (8YSZ) was used as an electrolyte material for high temperature SOFCs. A pre-ground 8YSZ powder (TZ-8YSZ, Tosoh) with high purity were used for producing pellets of magnitude 10 mm × 8 mm × 4 mm under the load of 12 kN/cm^2 and then sintered for 12 hrs at 1450 °C in high resistance furnace.

3.3. Diffusion couple preparation

The sintered 8YSZ (electrolyte) pellets were ultrasonically cleaned in acetone. The glass seal powder mixed with ethanol and then pasted on the outer layer of the pellets of 8YSZ. Initially to make the diffusion couples of glasses with 8YSZ electrolyte, the thermal treatment was given for 30 minutes to ensure incipient fusion of glass. The diffusion couples were heat treated at 850 °C in tubular furnace for 1000 h. The heat treated diffusion couples were mounted in the mold then mechanically polished with the diamond paste. These polished diffusion couples were used for interfacial and microstructural analysis.

3.4. Characterizations

The present samples were characterized using various techniques to check their applicability and suitability as sealing materials for SOFCs. The X-ray diffraction was used for nature of glass and glass ceramics. Differential thermal analysis (DTA) has been done to study thermal properties and stability of glasses. The CTE is very important parameter which has been measured by dilatometry. Micro structural analysis was carried out by scanning electron microscope (SEM). The particulars of these techniques are as follows:

3.4.1. Density measurement

Densities of the as prepared samples were calculated using xylene as the immersion medium by Archimedes' principle:

$$\rho_{sample} = \frac{W_a}{W_a - W_b} \times \rho_{xylene} \quad (3.1)$$

Where ρ_{sample} as sample density, ρ_{xylene} as xylene density, w_a as the weight of the sample in air and w_b as the weight of the sample in xylene. The xylene density at room temperature is 0.863 g/cm^3.Density was used to calculate the molar volume (V_m)of the as quenched glasses glasses using the following relation:

$$V_m = M/\rho \quad (3.2)$$

3.4.2. X-Ray Diffraction (XRD)

XRD study a non destructive method, which is the prime tool for characterizing the structure of crystalline materials, their crystallite size and disordering.

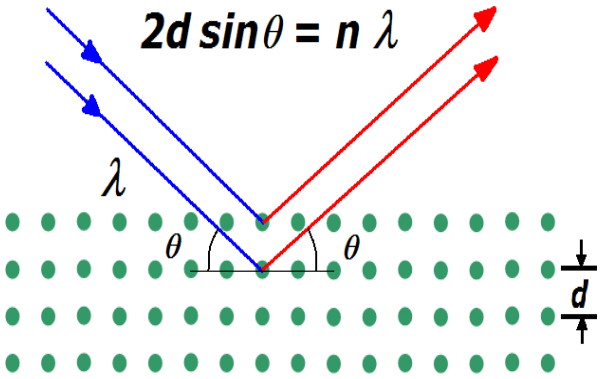

Figure 3.3: Diffraction of X-ray by planes of atom.

Monochromatic X-ray radiation was exposed on the quenched sample from which the reflected radiation is recorded by the analyzer. The XRD patterns were recorded at room temperature using PANalytical X'perts PRO MPD Diffractometer with Cu K_α radiation (λ = 1.54 Å) obtained from copper target using nickel to filter the undesired wavelengths. The XRD patterns of 2θ values were generally taken in the range of 10 degree to 80 degree at a 5 degree scan speed per minute. X-Ray diffraction by atom planes has shown in Figure 3.3.

3.4.3. Fourier transforms infrared (FTIR) spectroscopy

Infrared (IR) spectroscopy (figure 3.4), the most versatile spectroscopic method equipped to determine inorganic and organic substances. Absorbance of IR frequency is measured by positioning the sample in IR beam path. IR spectroscopic analysis aims to identify the presence of functional groups in the sample. With multiple accessories as sample holder in IR spectrometers we can characterize samples such as solids, liquids and gases. Some unknown spectrum of a material can be determined by comparing with known compounds.

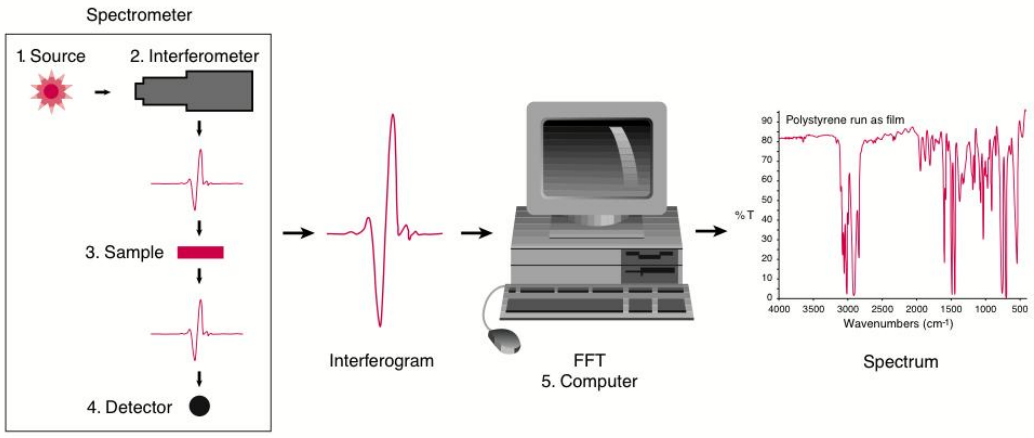

Figure 3.4: Fourier Transform Infra Red Spectroscopy.

An easily understandable FTIR spectrometer is exemplified in figure 3.4. The resultant IR analysis will be drafted wavelength or wavenumber in X-axis and absorbance or transmittance on Y-axis.

3.4.4. Differential thermal analysis (DTA)

DTA is a thermo-analytic technique, which gives information about the phase transformation behavior of the sample. In DTA, the thermal event of sample is observed with respect to the inert reference sample in heating or cooling cycle under identical conditions. Difference in temperature was correlated with respect to time. Transformation in the glasses like endothermic

or exothermic has been sensed in respect to the nobel reference where we can determine data's of conversion, such as T_g, T_c and T_m. In this thesis work differential thermal analysis of the powdered samples was done by DTA, Perking Elmer (Diamond TG/DTA) in nitrogen atmosphere (figure 3.5) using platinum crucibles at different heating rates from room temperature to 1000^{o}C.The endothermic peaks exhibit the T_g temperature and T_m of the glasses. On the other hand exothermic peaks denote crystallization of glasses.

Figure 3.5: Differential Thermal Analyzer (DTA).

The DTA sensitivity depends upon the heating rate. It is reduced with the slower rates because temperature for a particular event decreases with decreasing heating rate.

3.4.5. Dilatometry

Dilatometry is also called as thermal dilatometric analysis. It quantifies the dilation in a material during heating heated. This determines both expansion and shrinkage of a material during heating and cooling. A dilatometery set up is shown in Figure 3.6. It is used to determine the CTE, T_g, T_s T_c, T_m, phase transition and others. As the rise in temperature from RT to some elevated temperature (T) will lead to dilate the material from initial dimension L_o, Thus the change in dimension (longitudinal) will give the linear thermal expansion coefficient, which determined by following equation:

Figure 3.6: Dilatometer setup.

$$\alpha = (\Delta L_S / \Delta L_0) / (T - T_0) \quad (3.3)$$

Where, α is CTE and only true for the temperature between T_o to T.

The dilatometry of the glasses was done by Netzsch (DIL 402 PC) with heating rate 5 °C/min in open atmosphere. The range of temperature was from RT to T_g. Thermographs have been taken between temperature and % change in the length of a sample.

3.4.6. Scanning Electron Microscopy (SEM)

The SEM microscopy which can be used to magnify above 2000X is an electron microscope that captures images of a sample with a confined electron beam. The electrons intermingle with sample atoms and emit different signals which will be sensed and transformed in to microstructure of sample's surface topography by detector and the additional attachment EDS (Elemental Dispersive Spectroscopy) will give the information on chemical composition in percentage. The beam of electrons follows a raster pattern to scan sample's topography in-situ generates the image. SEM detects backscattered and secondary electrons that emerging from sample atoms, which are energized by the beam electrons. SEM reflects back-scattered electrons (BSE), secondary electrons (SE), characteristic X-rays, light (cathodoluminescence) (CL), specimen current and transmitted electrons which are collected by sensor for each signal.

Secondary electron imaging (SEI) is the most common practice that can produce very high-resolution images of sample surface which can detailed below 1 nm. Due to strong coherency in the electron beam, SEM micrographies have a large depth of field yielding a three-dimensional appearance in characterization that understands the sample structure. BSE are reflected by the sample via elastic scattering. BSE mode is used for analytical SEM in combine with characteristic X-rays, because the atomic number (Z) of atoms in specimen is strongly related to the intensity of BSE signal. BSE also contributes to elemental distribution in sample.

3.4.7 UV-Visible (UV/VIS) Spectroscopy

UV-Visible region wavelength is used in Ultra violet visible spectroscopy. Molecules at this region of spectrum experience transition in electronic states i.e. from excited state to ground state, in the meanwhile ground state to excited state transition happens due to absorbance of spectrum.

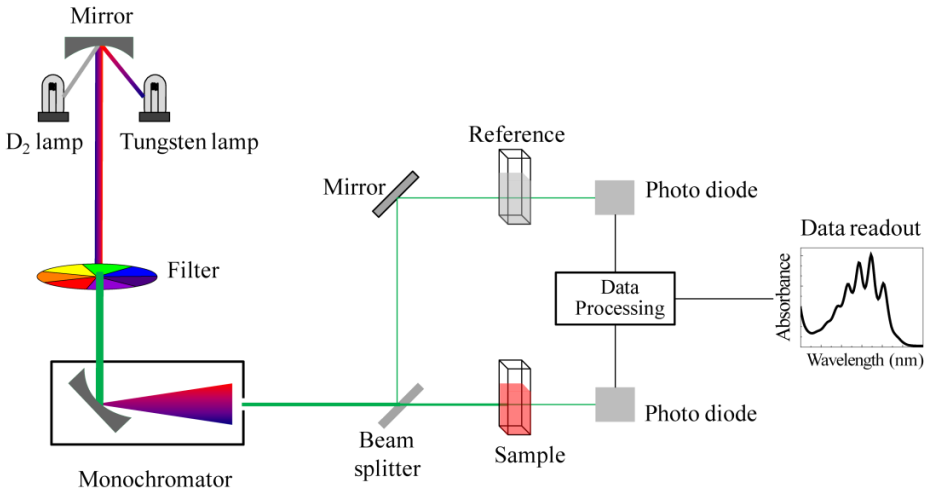

Figure 3.7: UV- Visible spectrophotometer.

This technique is reliable and uses for analyzing sample's emission, absorption and transmission of UV-Visible wavelength by matter are measured. EM radiations by atoms are quantified for transmission and absorbance by atoms. In this thesis, the spectrum of optical transmission in

samples were traced at RT using a double beam UV-Vis spectrometer (Model: Perkin Elmer 55) in the wavelength range of 200-800 nm. The data was analyzed for calculating the energy band gap of glasses. UV-Visible spectrometer is shown in figure 3.7.

CHAPTER 4 RESULTS AND DISCUSSION

4.1 Density and molar volume analysis

The densities, ionic concentration of alkaline earth ions, inter ionic concentration and molar volume of as quenched samples are listed in Table 4.1. The densities of all the quenched samples are measured by Archimedes principle. The molar volume of the prepared samples is calculated by the following equation:

$$V_m = M / \rho \quad (4.1)$$

Where, M is molar weight and ρ is density of glass. Ionic concentration of alkali earth metal ion (N) and their inter-ionic distance (R) can be calculated by the following relations:

$$N = (6.023 \times \text{mol\% of cation} \times \text{valency})/V_m \quad (4.2)$$

$$R = (1/N)^{1/3} \quad (4.3)$$

Table 4.1: Densities, molar volume of the glasses, ionic concentration of alkaline earth ions and their inter-ionic distance.

Sample ID	Density, ρ (g/cc)	Molar volume, V_m (cc/mol)	Ionic conc., N ($\times 10^{21}$/cc)	Inter-ionic distance, R (Å)
CZ-1	3.12	26.92	8.94	4.81
CZ-2	2.94	28.91	9.37	4.74
CZ-3	2.94	28.24	10.60	4.55
CZ-4	2.82	28.72	11.53	4.42

CZ-1 sample exhibits higher density in comparison to all other samples which is due to the higher molar mass of ZrO_2 as compared to CaO. Density of the as quenched samples is decrease with decreasing the amount of ZrO_2, as shown in Table 4.1. Density is generally an additive property. Hence, observed trend is associated with the replacement of denser ZrO_2 (5.68 gm/cm^3) with lighter CaO (3.35 gm/cm^3). CZ-4 glass exhibits higher molar volume indicated lower cross-

linking in this particular sample, whereas sample with lowest amount of ZrO_2 shows the highest ionic concentration with lowest inter-ionic distance in comparison to other samples. CZ-4 contains more concentration of CaO which is the possible reason for highest ionic concentration in this particular sample.

4.2 X-Ray diffraction (XRD) analysis

The prepared samples were studied with the help of X-Ray diffraction (XRD) technique. It was found that all samples were amorphous in nature due to the lack of sharp peaks in XRD patterns. XRD patterns of all prepared glasses are shown in Figure 4.1. The broad halos are observed in all prepared glasses between the angles i.e. 20 to 40°. In all the glasses, the broad halo shifted towards lower diffraction angles with the concentration of CaO. Interestingly, the XRD patterns do not show any second halo which indicates no phase separation in these glasses.

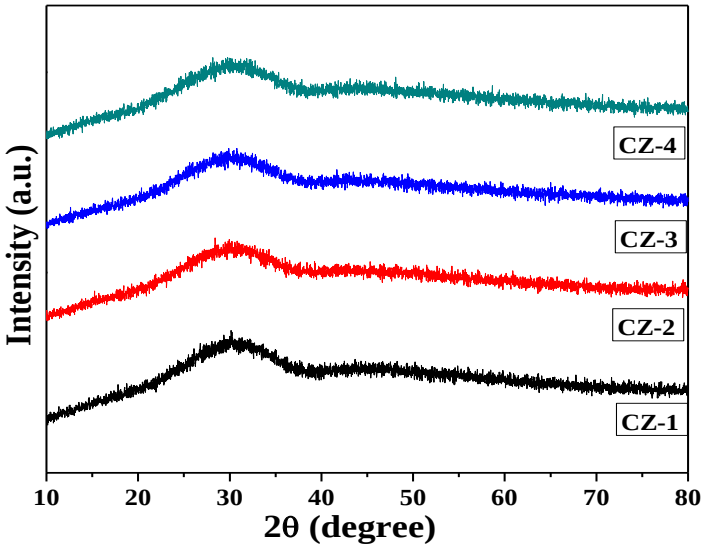

Figure 4.1: XRD patterns of the prepared samples.

4.3 FTIR analysis

FTIR spectra of all the glasses were recorded in the region 4,000-400 cm^{-1} at ambient temperature. The FTIR spectra of all the glasses are shown in Figure 4.2. It has been observed that silicate and borate groups play a dominant role in the spectra. The FTIR spectra of borate

based glasses exhibit three broad transmittance bands at 300-600 cm^{-1}, 600-800 cm^{-1} and 1300-1500 cm^{-1} [1, 2]. Although, alkaline earth metals are also present as modifiers in the glass network their presence is not observed in the FTIR spectra.

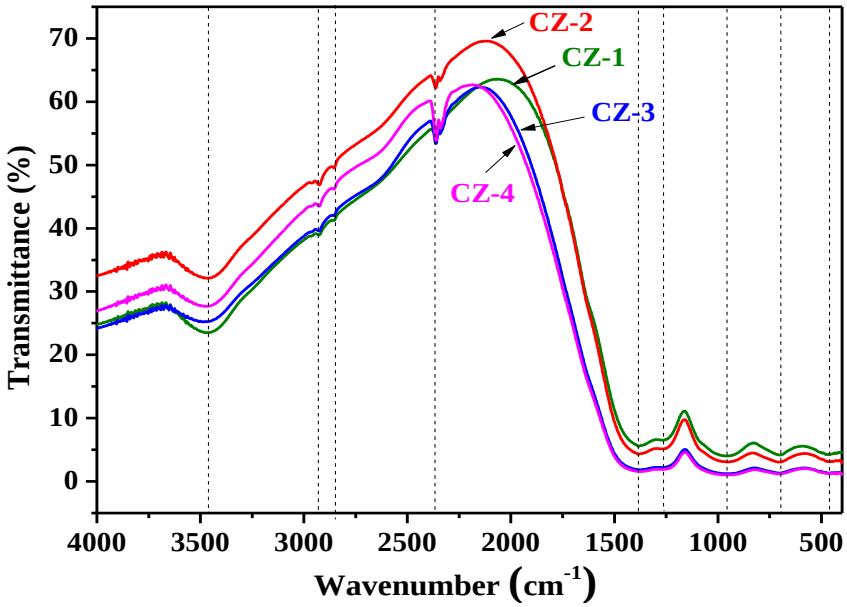

Fig. 4.2: FTIR spectra of all prepared glasses.

FTIR spectra of as prepared glasses show major IR bands at around1382 cm^{-1}, 1267 cm^{-1}, 955 cm^{-1}, 701 cm^{-1} and 476 cm^{-1} with some minor changes in the band intensities and peak positions with respect to each other. A small absorption band at about ~470 cm^{-1} is due to bending vibrations of SiO_4 tetrahedra [3]. The IR spectra of glasses exhibit a very small absorption band at 650-780 cm^{-1} which can be attributed to Si-O-Si stretching of bridging oxygen between tetrahedral [4,5]. Another band at 955 cm^{-1} could be assigned to the BO_4 stretching. Two medium intensity bands are also observed at around ~1268 cm^{-1} and ~1375 cm^{-1}. These bands can be attributed to boroxyl rings vibrations and BO_3 units vibrations, respectively. Apart from this, some bands appearing in the range ~2200-4000 cm^{-1} are due to OH and B-OH vibrations including the characteristic near infrared absorption bands of water [6]. It seems that the higher concentration of ZrO_2 help to increase the amount of SiO_4 tetrahedron in the present glasses. On

the other hand, the higher concentration of CaO increases both BO_4 and BO_3 structural units in the present glasses.

4.4 UV-Visible spectroscopy analysis

The optical band gap of sealing materials should be high. In other words, the insulator glass is required for the sealing purpose in SOFC's. In general, the optical band of the glasses decreases with increasing NBOs. The creation of NBOs depends on the concentrations in glass composition. This is because electrons associated with NBOs are loosely bound than that in BOs. With the increase in NBOs the ionicity of oxygen ions increases and top of the valence band is raised. As a result optical band gap decreases [7].

Table 4.2: Optical band gap of the all glasses.

Sample ID	**CZ-1**	**CZ-2**	**CZ-3**	**CZ-4**
Optical band gap (eV)	3.74	3.82	3.81	3.84

It has been observed that all glasses falls in the category of insulator as required for sealant. CZ-4 glass shows highest optical band gap (3.84 eV) as compared to other glasses. As reported by many researchers CaO is strong glass modifier than ZrO_2. The ZrO_2 can act as a modifier or former depending upon the initial concentration of ZrO_2. However, the present glasses do not follow this trend as given in Table 4.2. Similar trend has also been reported in other borosilicate glasses [8]. This may be attributed to the higher band gap of CaO (7.7 eV) is than ZrO_2 (5-7 eV).

4.5 Differential thermal analysis (DTA)

The glass transition temperature (T_g), crystallization temperature (T_c) and melting temperature (T_m) of glass samples are obtained from DTA using 25 °C/min heating rate. The results are summarized in Table 4.3. T_g, T_c and T_m values are low for CZ-4 glass as compared to other glasses.

Table 4.3: Characteristics temperatures of glasses obtained from DTA.

Sample ID	T_g(°C)	T_c(°C)	T_m(°C)	T_c-T_g (°C)
CZ-2	756	896	926	140
CZ-3	752	862	904	120
CZ-4	745	814	857	69

This behavior of glasses can be attributed to large size difference between Ca^{2+} (1.14 Å) and Zr^{4+} (0.86Å) within the glass matrix [9, 10]. On the other hand, CaO acts as a modifier in the present glass systems which create the higher NBOs. These NBOs break the glass structure resulting decrease in the T_g. According to Lasocka, the thermal stability of glasses can be obtained by the difference between T_g and T_c. Higher the difference more resists the devetrification of glasses. The higher difference is observed in CZ-2 glass. It means that CZ-2 is thermally more stable as compared to other glasses. These results support that ZrO_2 might acts as glass former. Conclusively, the higher concentration of the ZrO_2 decreases the NBOs which increase the T_g, T_c, T_m and thermal stability of glasses.

4.6 Coefficient of thermal expansion (CTE)

The expansion of glass can be determined by taking into consideration the attraction between ions as follows [11]:

$$F = 2Z/d^2 \qquad (4.4)$$

Where F is force of attraction, Z is charge of positive ions and d is the distance between positive and negative ions. As the time duration of heat-treatment increases, the amplitude of thermal vibrations within the glass network also gets enhanced. Coefficient of thermal expansion is due to the asymmetry potential well in the system [12]. Moreover, in asymmetric potential well, the

atoms spend more time at r >r_o, where r_o is the equilibrium distance at absolute zero temperature. This may subsequently decrease the attraction between ions and increase the bond length leading to expansion of glass network. The CTE values obtained from a dilatometer as a function of temperature was observed for all the glasses. The measurements for the CTE were carried out from room temperature up to temperature which is slightly below the glass softening temperature (T_s). The CTE of the as prepared glasses is given in Table 4.4.

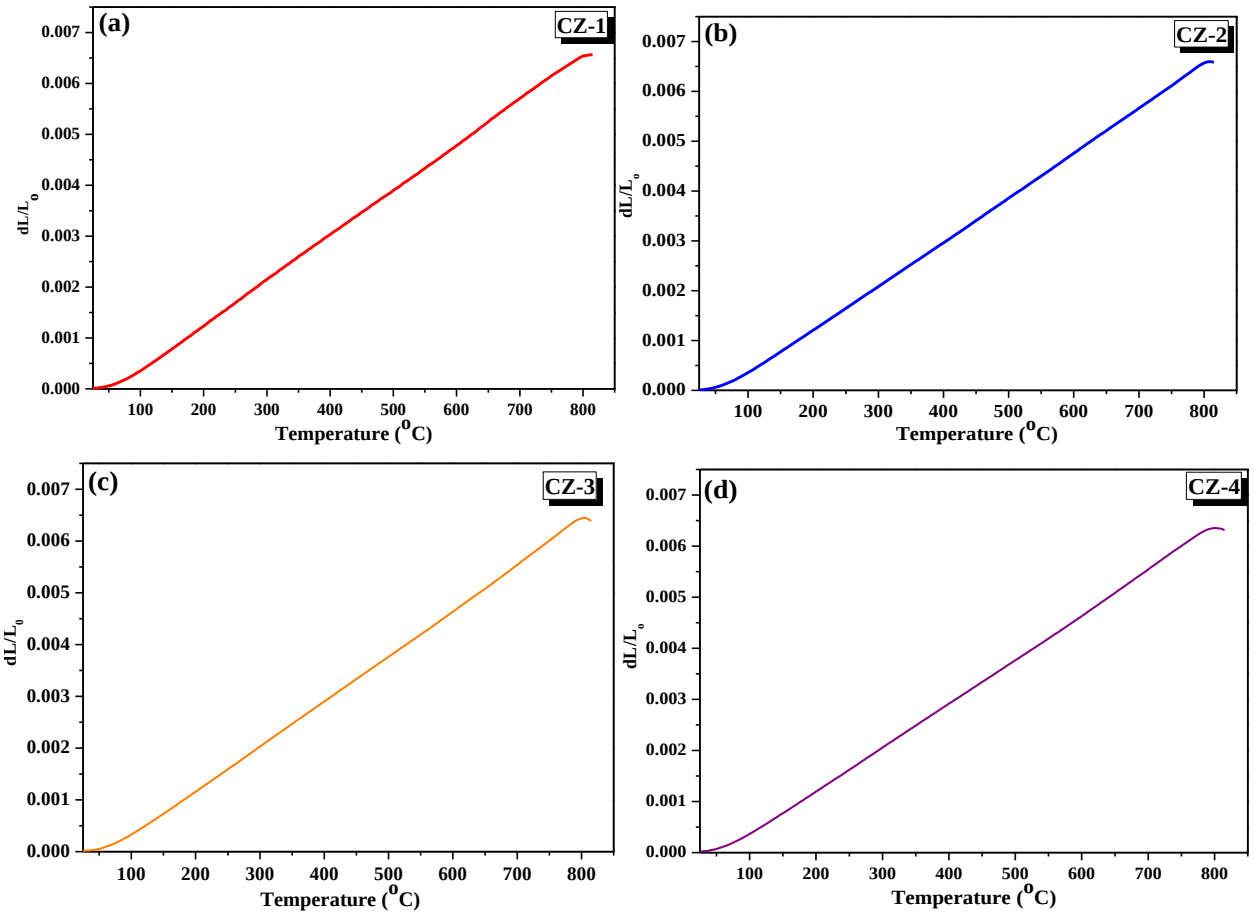

Figure 4.3: Dilation curve for glasses (a) CZ-1 (b) CZ-2 (c) CZ-3 (d) CZ-4.

CTEs of the glasses are calculated with the help of taking the slope of the linear portion of the dilatometry curve (Figure 4.3) at different temperatures ranges [13]. CTE of as prepared glasses falls in the range, which is required for a sealant using in solid oxide fuel cell.

Table 4.4: Calculated CTE from the linear part of the curve.

Sample ID	CTE ($10^{-6}/^{\circ}C$) (Between 400-600 ^{o}C)	CTE ($10^{-6}/^{\circ}C$) (Between 500-700 ^{o}C)	CTE ($10^{-6}/^{\circ}C$) (Between 600-800 ^{o}C)
CZ-1	8.71	9.05	8.78
CZ-2	8.97	9.02	9.06
CZ-3	8.66	8.88	9.03
CZ-4	8.59	8.89	8.61

The CTE of all the as quenched glasses are in the range of ~9×10^{-6}/°C which is very near to the coefficient of thermal expansion of YSZ (10.5×10^{-6}/°C). It is well reported in the literature that the difference in CTE between 1-1.5×10^{-6}/°C is acceptable among various components of solid oxide fuel cell [14]. The CTE is slightly different in different temperature range. However, their values are in permissible range which is required for SOFC.

4.7 SEM analysis

The microstructure of diffusion couple were taken after exposing at 850 °C for 1000 h. Before SEM measurement, the diffusion couples were ground, polished and cleaned ultrasonically. The SEM images confirm that strong bond have been formed at the interface of glasses and electrolyte (8YSZ). The experiments have been conducted in an oxidizing atmosphere for interfacial study. The chemical reaction at the interface is controlled by the diffusion process. Figures 4.4 and 4.5 show the SEM micrograph of glass/8YSZ couples heat treated at 850 °C for 1000 h. The SEM is focused on the central part of the interface. It has been observed that all the diffusion couples formed a good interface. However, interface shows very low residual porosity within glass, which is attributed to small CTE mismatch between glass and 8YSZ. Diffusion of the calcium, silicon from glass side to 8YSZ has been detected by point analysis of energy dispersive spectroscopy (EDS) of joint region. However, some diffusion of yttrium from 8YSZ

side to glass also has been detected. Hence, relatively better joining was observed between glass and electrolyte. The absence of crack near the interface indicates good chemical and physical compatibility between 8YSZ and glass seals. As shown in the figures 4.4 and 4.5, the smooth and porosity free interface is observed in case of CZ-1/8YSZ diffusion couple. As CaO increases, the thermal stability of glasses decreases (as discussed in DTA section 4.5). The replacement of CaO by ZrO_2 leads to smooth interface with minimum interfacial reaction at the interface. Among all the glasses, CZ-1 glass is more compatible with 8YSZ than other glasses.

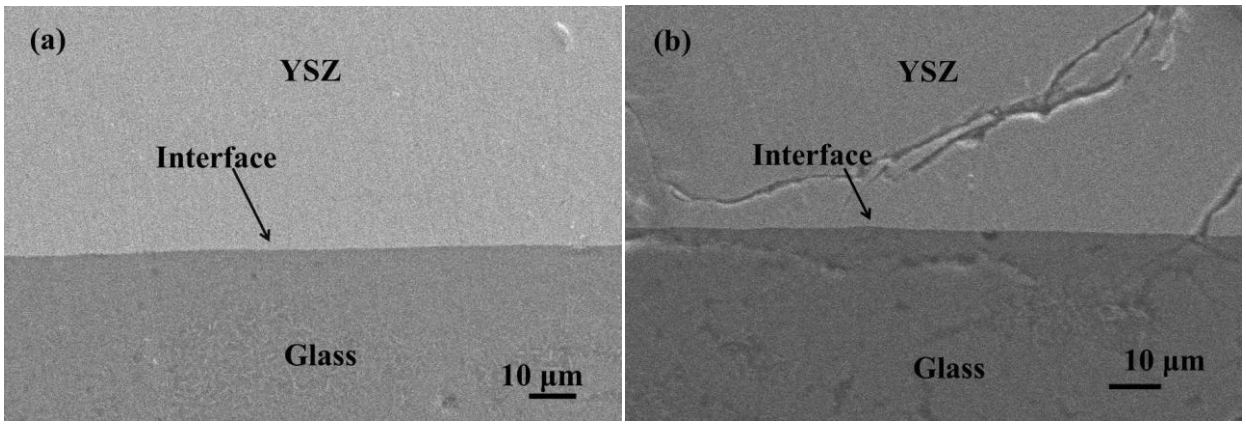

Figure 4.4: Diffusion couple at 850 °C for 1000 h (a) CZ-1 (b) CZ-2.

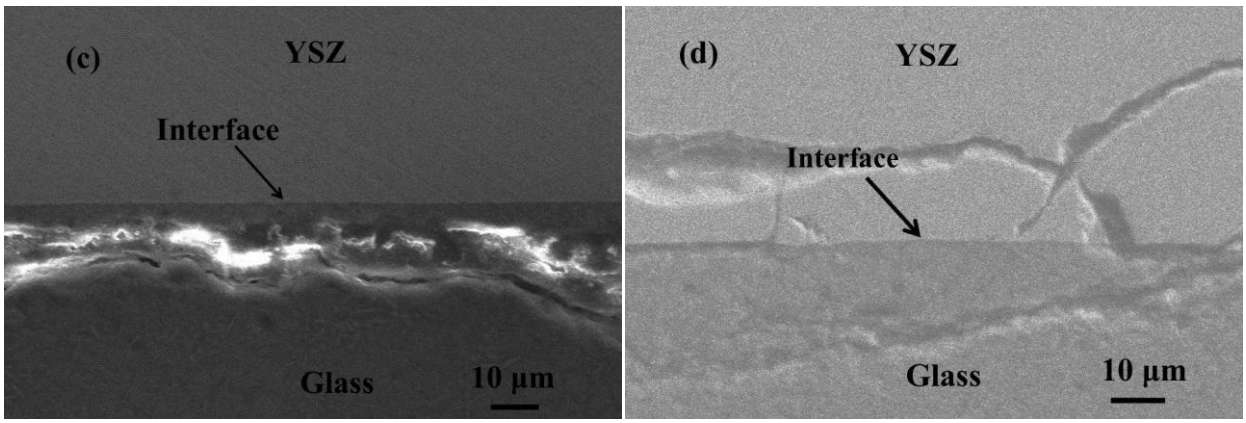

Figure 4.5: Diffusion couple at 850 °C for 1000 h (a) CZ-3 (b) CZ-4.

References:

1. S. Singh, K. Singh, J. Mol. Struct.1081 (2015) 211.
2. G. Kaur, M. Kumar, A. Arora, O. P. Pandey, K. Singh, J. Non-Cryst. Solids 357 (2011) 858.
3. Q. Williams, E. Knittle, J. Phys. Chem. Solids 57 (1996)417.
4. S. Simon, I. Ardelean, S. Filip, I. Bratu, I. Cosma, Solid State Commun. 116 (2000)83.
5. M. Bosca, L. Pop, G. Borodi, P. Pascuta, E. Culea, J. Alloys Compd. 479 (2009)579.
6. F. Urbach, Phys. Rev. 92 (1953) 1324.
7. C. Rajyasree, D. K. Rao, J. Non-Cryst. Solids 357 (2011) 836.
8. S. Singh, G. Kalia, K. Singh, J. Mol. Struct. 1086 (2015) 239.
9. F. Tietz, Ionics 5 (1999) 129.
10. M. K. Mahapatra, K. Lu, Mat. Sci. Engg. R 67 (2010) 65.
11. V. Raghvan, Materials Science and Engineering (5^{th} edition 2008) p-74.
12. S. Ghosh, P. Kundu, A. D. Sharma, R. N. Basu, H. S. Maiti, J. Euro. Cera. Soc. 8 (2008) 69.
13. E. S. Lim, B. S. Kim, J. H. Lee, J. J. Kim, J. Euro. Cera. Soc. 27 (2007) 819.
14. C. T. Moynihan, S. K. Lee, M. Tatsumisago, T. Minami, Thermochim. Acta. 280 (1996) 153.

CHAPTER 5 CONCLUSION AND FUTURE SCOPE

5.1 Conclusion

Yttrium and zirconium contained calcium borosilicate glasses were prepared by melt quench technique and then characterized by XRD, FTIR, DTA, dilatometry, UV-Visible spectroscopy and SEM with EDS techniques. Density of the glasses decreases with decrease in ZrO_2 concentration. All the samples are amorphous in nature without having any phase separation. FTIR spectra of all the glasses confirm the presence of silicate and borate groups in the glasses. Optical band gaps of the glasses fall in the insulator region with values > 3.74 eV. The CTE of the present glasses is in the required range for SOFCs applications. It is comparable to the CTE of other components of SOFCs, which makes these glasses suitable for SOFCs applications. The T_g, T_c and T_m increases with concentration of ZrO_2. The diffusion couples of these glass sealants with electrolyte (8YSZ) were heat treated at 850 °C for 1000 h. The smooth interface is formed between all the glasses/8YSZ diffusion couples. All glass sealants exhibit good hermiticity and structural integrity with electrolyte even after prolonged heat treatment except CZ-4. Present glasses formed strong and crack free interface with 8YSZ.

5.6 Future scope

The interfacial study between glass and other components of SOFCs like cathode, anode and interconnect will be beneficial for their applicability as a sealant. These glass sealants can be tested in real SOFC conditions like reducing atmosphere, longer duration with variable thermal cycle. Interfacial reaction kinetics shall be investigated with the different components of SOFC, to monitor the interfacial stability.